TECHNICAL

Non-invasive assessment of mesenteric hemodynamics in patients with suspected chronic mesenteric ischemia using 4D flow MRI

Grant S. Roberts[1] · Christopher J. François[2] · Jitka Starekova[2] · Alejandro Roldán-Alzate[2,3] · Oliver Wieben[1,2]

Abstract

Purpose Chronic mesenteric ischemia (CMI) is a rare disease with a particularly difficult diagnosis. In this study, 4D flow MRI is used to quantitatively evaluate mesenteric hemodynamics before and after a meal in patients suspected of having CMI and healthy individuals.

Methods Nineteen patients suspected of CMI and twenty control subjects were analyzed. Subjects were scanned using a radially undersampled 4D flow MR sequence (PC-VIPR). Flow rates were assessed in the supraceliac (SCAo) and infrarenal aorta, celiac artery, superior mesenteric artery (SMA), left and right renal arteries, superior mesenteric vein (SMV), splenic vein, and portal vein (PV) in a fasting state (preprandial) and 20 min after a 700-kcal meal (postprandial). Patients were subcategorized into positive diagnosis (CMI+, $N = 6$) and negative diagnosis (CMI−, $N = 13$) groups based on imaging and clinical findings. Preprandial, postprandial, and percent change in flow rates were compared between subgroups using a Welch t test.

Results In controls and CMI− patients, SCAo, SMA, SMV, and PV flow increased significantly after meal ingestion. No significant flow increases were observed in CMI+ patients. Percent changes in SMA, SMV, and PV flow were significantly greater in controls compared to CMI+ patients. Additionally, percent changes in flow in the SMV and PV were significantly greater in CMI− patients compared to CMI+ patients.

Conclusions 4D flow MRI with large volumetric coverage demonstrated significant differences in the redistribution of blood flow in SMA, SMV, and PV in CMI+ patients after a meal challenge. This approach may assist in the challenging diagnosis of CMI.

Keywords 4D flow MRI · Phase contrast · Radial undersampling · Hemodynamics · Atherosclerosis · Chronic mesenteric ischemia

Introduction

Chronic mesenteric ischemia (CMI) is a disease caused by underlying stenotic and occlusive vessel diseases typically affecting the proximal portions of the primary mesenteric vessels—the celiac artery (CA), superior mesenteric artery (SMA), and inferior mesenteric artery (IMA)—resulting in inadequate blood flow to the small intestine following meal ingestion [1]. While mesenteric artery stenoses are relatively common in aging populations, CMI is rare because of collateral pathways within the mesenteric vasculature that often compensate for reduced blood flow [2]. In patients with CMI, the normal increase in mesenteric blood flow after meal consumption (postprandial hyperemia) is stunted causing dull, postprandial abdominal pain 15–60 min after meal ingestion with pain continuing up to 4 h. This subsequently leads to fear of food, severe weight loss, malnutrition, and can eventually progress to acute-on-CMI which is associated with a high mortality rate [3]. Operative and endovascular interventions are treatment options that are often successful [4], but proper diagnosis of CMI remains

✉ Oliver Wieben
owieben@wisc.edu

1 Department of Medical Physics, University of Wisconsin - Madison, Madison, WI, USA

2 Department of Radiology, University of Wisconsin - Madison, Madison, WI, USA

3 Department of Mechanical Engineering, University of Wisconsin - Madison, Madison, WI, USA

🌐 Springer

challenging and requires a high index of clinical suspicion, typically raised on the basis of presenting symptoms, presence of mesenteric artery stenoses from imaging findings, coexistence of cardiovascular risk factors, and exclusion of other potential pathologies as summarized in the *European CMI guidelines* [5].

If clinical findings strongly suggest CMI, contrast-enhanced CT angiography (CTA) of the abdomen is usually the first diagnostic exam of choice because it can identify and locate regions of stenosis and occlusion, as well as simultaneously exclude other abdominal pathologies [6–8]. Contrast-enhanced magnetic resonance angiography (CE-MRA) may also be used, with studies demonstrating both high sensitivity and specificity in detecting proximal mesenteric lesions [9–11]. However, CTA and CE-MRA lack functional information regarding mesenteric blood flow, the underlying physiological component of the disease. Duplex sonography has shown some success in characterizing the extent of stenoses in patients suspected of CMI and has demonstrated that evaluating blood hemodynamics before and after a meal challenge can provide additional diagnostic information [12–14]. However, sonography is not always feasible due to technical limitations, such as bowel gas overlying vessels of interest, excess adipose tissue, variable anatomy, and operator dependence [15].

Two-dimensional time-resolved phase-contrast magnetic resonance imaging (2D PC-MRI) has shown promise in non-invasively screening patients with suspected CMI by measuring volumetric blood flow rates in mesenteric vasculature to evaluate postprandial hemodynamic responses [16–19]. Using 2D PC-MRI, it was first shown by Li et al. [16] that postprandial flow augmentation in the SMA was reduced proportionally to the severity of atherosclerosis in mesenteric vessels. A subsequent study by Burkart et al. [17] used 2D PC-MRI to prospectively evaluate suspected CMI patients by measuring volumetric blood flow rates in the superior mesenteric vein (SMV) before and after a meal; results showed a drastically impaired hemodynamic response in the SMV in patients with true CMI compared to those who were symptomatic (with and without stenosis) but did not have CMI per clinical follow-up angiography studies. A second study by Li et al. [18] reinforced these findings by showing that reduced postprandial flow augmentation occurs in both the SMV and SMA in patients with CMI. Despite these encouraging results, 2D PC-MRI is cumbersome in that it requires flow measurements in multiple vessel segments, which are patient-specific based on individual anatomy. Hence, an additional high-quality MR angiogram is required to identify the major vessels and potentially involved collaterals so that imaging planes can be placed perpendicular to vessel paths of interest. This leads to increased scan times and variability due to operator involvement.

Volumetric, time-resolved PC-MR with three-dimensional velocity encoding (4D flow MRI) has emerged as a compelling approach that can simultaneously interrogate large vascular territories for 3D MRA and functionally assess mesenteric hemodynamics all in one scan session [20, 21]. Due to the volumetric nature of the acquisition, any vessel within the 3D field of view can be retrospectively analyzed without additional scan time penalty. A recent study using 4D flow MRI demonstrated the feasibility of a meal challenge in evaluating hepatic and mesenteric blood flow responses in portal hypertension patients [22]. In this work, we use a similar 4D flow MRI approach to quantify the effects of a meal challenge in patients suspected of CMI and in healthy control subjects, thereby taking advantage of the large volumetric coverage to comprehensively assess the flow response in multiple mesenteric vascular segments.

Methods

Subject population

In this Health Insurance Portability and Accountability Act (HIPAA)-compliant and Institutional Review Board (IRB)-approved retrospective study, 21 consecutive patients (13 females, mean age: 47.5 years [21–86], mean weight: 69.2 kg) with a suspicion of CMI were scanned according to our clinical CMI protocol. Studies were performed between March 2012 and August 2019 on patients referred from vascular surgery or gastroenterology based on a clinical presentation typical of CMI (including postprandial abdominal pain, weight loss, adapted eating patterns, diarrhea, and nausea), imaging findings, or both (see Appendix Tables 4, 5). Note that the absence of one or more symptoms did not exclude the possibility of CMI. Of the 21 patients, 4D flow data were successfully obtained in 19 patients (11 females, mean age: 50.1 years [21–86], mean weight: 69.4 kg). Two cases could not be analyzed due to high levels of noise resultant from acquisition errors and were excluded from the study. Patients were subcategorized into positive (CMI+) and negative (CMI−) groups based on imaging and/or clinical findings. Patients were classified as CMI+ if imaging demonstrated significant stenoses ($\geq 50\%$) in 2 or more primary vessels [9], or if clinical findings strongly suggested CMI and mesenteric revascularization successfully relieved a patient's symptoms [2]. Classification of CMI+ was only made after excluding other alternative diagnoses. Image interpretation and clinical diagnoses were performed by a trained cardiovascular radiologist (CJF) with 17 years of experience. Twenty control subjects (8 females, mean age: 44.4 years [19–73], mean weight: 80.2 kg) underwent the same CMI protocol as the patient cohort and were analyzed retrospectively. Control subjects were defined as individuals

asymptomatic of CMI or other vascular disease with no mesenteric artery stenosis.

Imaging protocol

Control subjects were scanned on a clinical 3.0T scanner (Discovery MR750, GE Healthcare, Waukesha, WI) with a 32-channel phased array torso coil (NeoCoil, Pewaukee, WI). Subjects from the CMI+ and CMI− groups were scanned on either a clinical 1.5T or 3.0T scanner (Signa HDX, Optima 540w, or Discovery MR750, GE Healthcare, Waukesha, WI) with various torso coils (8-channel, 12-channel, 24-channel, and 32-channel) based on scanner and coil availability at the time of examination. As part of the CMI protocol, 4D flow MRI was performed both before and after a standardized meal challenge. An initial preprandial scan was performed after at least 5 h of fasting. Following previous study designs [17–19, 22], subjects ingested 474 mL of Ensure Plus (700 kcal, 56% carbohydrates, 29% fats, 15% protein; Abbott Laboratories, Columbus, OH) followed by a second postprandial scan 20 min after meal ingestion. Twenty minutes was chosen to allow for sufficient arterial and venous blood flow responses to be observed [22, 23].

4D flow MRI was performed using a 5-point, radially undersampled acquisition (Phase Contrast Vastly undersampled Isotropic Projection Reconstruction, PC-VIPR) that provides high spatial resolution, increased motion robustness, and retrospective gating flexibility within a reasonable scan time [24, 25]. Complete volumetric coverage of the abdomen was acquired, centered over the celiac axis with the following imaging parameters: TR = 6.6–8.3 ms; TE = 1.9–2.7 ms; tip angle = 14°; number of projections = 11,000; acquired isotropic resolution = 1.25 mm; reconstructed imaging volume = 32 cm^3; scan time = 11 min. Intravenous contrast agents containing 0.03 mmol/kg of gadofosveset trisodium (Lantheus, North Billerica, MA) were administered immediately before the preprandial scan in 17 controls and 19 patients. Three control subjects and one patient did not receive contrast agents due to contraindications or refusal. The velocity encoding (V_{enc}) was set to 100 cm/s for the preprandial scan and was increased to 120 cm/s for the postprandial scan to account for anticipated increases in mesenteric blood velocities. During image acquisition, ECG and respiratory monitoring were performed to allow for retrospective cardiac and respiratory gating during reconstruction.

Data analysis and flow measurements

Reconstruction was performed offline yielding time-resolved and time-averaged magnitude, complex difference, and 3-directional velocity data. Retrospective respiratory gating was performed with a 50% acceptance window for all data (expiration phase). All time-resolved data were reconstructed into 14 cardiac time frames using temporal view sharing [26]. Background phase correction was performed on all datasets by fitting a third-order polynomial to phase in stationary tissue, defined by semi-automatically thresholding time-averaged magnitude and velocity data [27]. Time-averaged complex difference data were exported to Mimics (Materialize, Leuven, Belgium, RRID:SCR_012153) for semi-automatic vessel segmentation (global thresholding plus region growing) in order to create 3D PC angiogram masks, shown in Fig. 1.
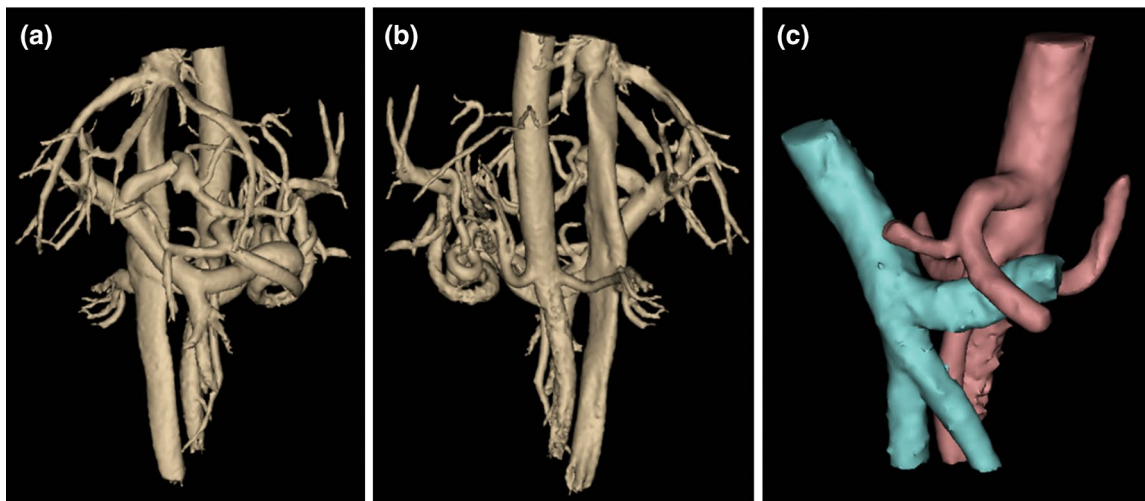

Fig. 1 Phase contrast (PC) angiograms of the mesenteric vasculature created from 4D flow MRI complex difference data. Anterior (**a**) and posterior (**b**) views of the segmented angiogram for a healthy (61-year-old, male) control subject. Note the high vascular detail. "Trimmed" PC angiogram from the same subject, including only relevant venous (blue) and arterial (red) vasculature needed for quantitative analysis (**c**)

Angiograms and time-resolved velocity data were exported to Ensight (ANSYS, Canonsburg, PA) for visualization of blood flow patterns and interactive 2D plane placement for flow analysis. Color-coded vector streamline images and particle traces were created in Ensight to visualize time-resolved flow patterns (Fig. 2). 2D cut-planes were manually placed in vessels of interest perpendicular to the direction of the vessel for quantitative flow analysis. Flow analysis was performed in 6 arteries: superior mesenteric artery (SMA), celiac artery (CA), supraceliac aorta (SCAo), infrarenal aorta (IRAo), right renal artery (RRA), left renal artery (LRA), as well as 3 veins: superior mesenteric vein (SMV), splenic vein (SV), and portal vein (PV). All cut-planes were placed at least 2 vessel diameters away from either a confluence or bifurcation to avoid regions of highly disturbed flow due to entrance effects. In some datasets, certain vessel segments could not be well visualized on the PC angiogram due to either an insufficient size of the imaging volume, vessel occlusions, or very slow flows. In these cases, flow analysis was not performed.

Data from the 2D cut-planes were exported to a customized software package [28] where manual, time-resolved segmentation was performed on all vessels (Fig. 2a inset) to account for pulsatile vessel motion during the cardiac cycle. All planes were visually inspected to ensure that velocity aliasing had not occurred. Volumetric flow rates were calculated by multiplying average in-plane velocity by total cross-sectional vessel area. Average volumetric flow rates were determined by taking the mean volumetric flow rate over the cardiac cycle (mL/cycle) and multiplying this value by the subject's heart rate to obtain volumetric flow rates in units of time (mL/s). All flow rates were then normalized by the subject's body weight (kg) to avoid influence of body size on flow rate magnitudes as has been done in similar studies [17–19, 29–31]. For each subject, average pre- and postprandial volumetric flow rates, as well as the percent change in flow values, were calculated for all visualized vessels. Group-averaged preprandial, postprandial, and percent change in flow values were calculated for all vessels by averaging values over all subjects in each of the three subgroups.

Internal consistency measurements

Internal consistency of flow measurements was assessed using conservation of flow in the measured arterial and venous segments. Conservation of flow would require the difference between SCAo and IRAo flow ($\bar{Q}_{\text{loss}}$) to be approximately equal to the sum of the flow of vessels exiting between these two arterial segments ($\bar{Q}_{\text{branch}}$), as visualized in Fig. 2a and represented in Eq. (1):

$$\bar{Q}_{\text{loss}} = \bar{Q}_{\text{SCAo}} - \bar{Q}_{\text{IRAo}} \approx \bar{Q}_{\text{CA}} + \bar{Q}_{\text{SMA}} + \bar{Q}_{\text{RRA}} + \bar{Q}_{\text{LRA}} = \bar{Q}_{\text{branch}} \tag{1}$$

An analogous conservation law holds for venous flow measurements:

$$\bar{Q}_{\text{PV}} \approx \bar{Q}_{\text{SV}} + \bar{Q}_{\text{SMV}} \tag{2}$$

As a means of comprehensively assessing internal consistency of flow, correlation analysis was used to compare measured arterial loss ($\bar{Q}_{\text{loss}}$) to measured flow from branching mesenteric arteries ($\bar{Q}_{\text{branch}}$) and similarly for flow in the portal vein ($\bar{Q}_{\text{PV}}$) and the sum of flow in the splenic and superior mesenteric veins ($\bar{Q}_{\text{SV}} + \bar{Q}_{\text{SMV}}$). Datasets with missing vessel segments (e.g., due to vessel location outside imaging volume, occlusions, or imaging artifacts) were excluded from this analysis.

Statistical analysis

Within each subgroup, flow rate differences before and after a meal were compared using a two-tailed paired *t* test.

Fig. 2 Velocity color-coded pathlines (**a**) soon after systole in the arterial vasculature of a healthy (61-year-old, male) control subject. Velocity color-coded streamline images (**b**) in the venous system soon after systole for the same control subject. 2D cut-planes (**a**, **b**) are shown for all mesenteric vessels being quantitatively analyzed. Inset image shows time-resolved, manual segmentation of the CA in a customized software package
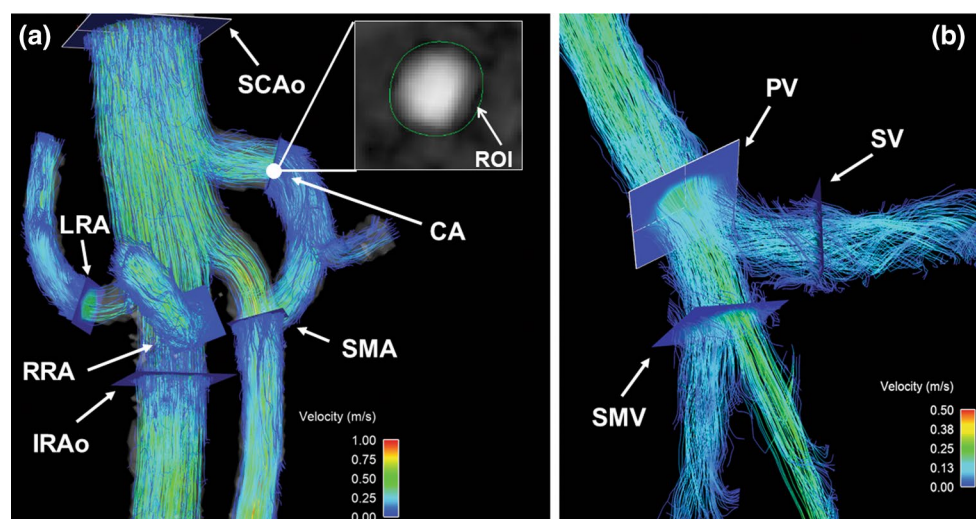
Additionally, preprandial, postprandial, and percent change in flow values were compared between subgroups using a two-tailed Welch t test. For all statistical tests, $p < 0.05$ was chosen to reflect statistical significance. Cohen's d effect sizes [32] were reported in conjunction with p values. For flow consistency analysis, all complete preprandial and postprandial datasets from each subgroup were combined and coefficients of determination (R^2 values) were obtained for arterial and venous measurements.

Results

Flow analysis

After subject categorization, the cohorts consisted of 13 CMI− patients (7 females, mean age: 45.1 years [21–86], mean weight: 73.5 kg) in which findings did not support the diagnosis of CMI and 6 CMI+ patients (4 females, mean age: 58.6 years [35–80], mean weight: 62.4 kg), in which findings strongly suggested CMI. In 4 CMI+ subjects, revascularization successfully relieved presenting symptoms and in 2 CMI+ subjects, imaging demonstrated 2 or more stenoses/obstructions ($> 50\%$ narrowing). Details of presenting symptoms, diagnostic findings, revascularization procedures, and clinical follow-ups are provided in the Appendix for CMI+ subjects (Table 4) and CMI− subjects (Table 5). A summarized list of clinically relevant comorbidities, risk factors, and presenting symptoms is provided in Table 1.

In some subjects, vessels were not visualized in the PC angiograms. Between all 78 preprandial and postprandial datasets, this occurred 2 times in the SCAo, 5 times in the

Table 1 Comorbidities, risk factors, and presenting symptoms of CMI+ and CMI− subjects

	CMI+ ($N = 6$)	CMI− ($N = 13$)
Relevant comorbidities & risk factors N (%)		
Hypertension	6 (100%)	7 (54%)
Obesity	2 (33%)	8 (62%)
Smoking history	5 (83%)	8 (62%)
Dyslipidemia	3 (50%)	3 (23%)
Esophageal reflux	2 (33%)	3 (23%)
Pancreatic disease	1 (17%)	2 (15%)
Vasculitis	1 (17%)	1 (8%)
Presenting symptoms N (%)		
Postprandial abdominal pain	4 (67%)	9 (69%)
Nausea	3 (50%)	6 (46%)
Weight Loss	3 (50%)	6 (46%)
Vomiting	1 (17%)	3 (23%)
Diarrhea	1 (17%)	1 (8%)

IRAo, 2 times in the LRA, 6 times in the RRA, 4 times in the CA, 2 times in the SMV, 5 times in the SV, and 2 times in the PV, leaving 59 arterial and 69 venous datasets for consistency analysis. The SMA was visualized on all image sets. Average weight-corrected pre- and postprandial volumetric flow rates for each group are shown in Table 2. Average percent changes in flow for each group are given in Table 3 and visualized in Fig. 3.

SCAo and IRAo

In control subjects, SCAo blood flow increased significantly 20 min after a meal ($p = 5.62e-05$, Cohen's $d = 0.381$) as did blood flow in the CMI− group ($p = 0.003$, $d = 0.543$). In contrast, the CMI+ group showed no significant increase in blood flow after the meal ($p = 0.473$). Absolute preprandial and postprandial SCAo flow values were not significantly different between any group. Furthermore, percent change in SCAo flow was not significantly different among groups. Likewise, IRAo flow analysis demonstrated no significant differences in preprandial or postprandial IRAo flow between groups. There was also no significant difference in percent change in IRAo blood flow between groups.

Table 2 Average volumetric flow rates (mL/min/kg)

Vessel		Control	CMI−	CMI+
SCAo	Pre-flow (mL/min/kg)	48.2 ± 17.6	42.0 ± 12.8	43.2 ± 18.9
	Post-flow (mL/min/kg)	55.3 ± 19.9	49.5 ± 14.9	48.0 ± 32.7
IRAo	Pre-flow (mL/min/kg)	15.5 ± 7.81	16.5 ± 6.39	19.7 ± 3.85
	Post-flow (mL/min/kg)	14.0 ± 6.15	17.3 ± 5.33	20.2 ± 7.36
LRA	Pre-flow (mL/min/kg)	5.00 ± 3.40	5.92 ± 2.54	4.60 ± 3.61
	Post-flow (mL/min/kg)	4.94 ± 2.91	5.79 ± 2.27	4.29 ± 4.43
RRA	Pre-flow (mL/min/kg)	4.85 ± 2.42	5.43 ± 2.25	7.18 ± 6.38
	Post-flow (mL/min/kg)	5.21 ± 2.72	5.17 ± 2.04	5.87 ± 6.28
SMA	Pre-flow (mL/min/kg)	5.97 ± 3.15	7.35 ± 3.73	8.84 ± 4.36
	Post-flow (mL/min/kg)	11.1 ± 5.00	10.6 ± 4.66	11.2 ± 6.32
CA	Pre-flow (mL/min/kg)	11.8 ± 7.88	**7.00 ± 3.79**	7.29 ± 3.47
	Post-flow (mL/min/kg)	11.0 ± 7.00	7.08 ± 4.80	8.11 ± 3.62
SMV	Pre-flow (mL/min/kg)	6.61 ± 2.66	6.24 ± 3.62	*11.4 ± 3.79*
	Post-flow (mL/min/kg)	14.2 ± 4.56	14.2 ± 3.80	17.7 ± 9.87
SV	Pre-flow (mL/min/kg)	6.52 ± 4.18	6.12 ± 3.82	5.80 ± 2.33
	Post-flow (mL/min/kg)	5.80 ± 2.52	5.87 ± 4.17	4.80 ± 1.76
PV	Pre-flow (mL/min/kg)	14.1 ± 5.57	13.2 ± 4.50	17.8 ± 5.22
	Post-flow (mL/min/kg)	20.6 ± 5.91	21.3 ± 4.88	22.3 ± 10.3

Volumetric flow rates are expressed as mean ± 1 standard deviation. Bold indicates statistical significance ($p < 0.05$) compared to controls. Italic indicates statistical significance ($p < 0.05$) between CMI+ and CMI− groups

SCAo supraceliac aorta, *IRAo* infrarenal aorta, *LRA* left renal artery, *RRA* right renal artery, *SMA* superior mesenteric artery, *CA* celiac artery, *SMV* superior mesenteric vein, *SV* splenic vein, *PV* portal vein

Table 3 Average percent change in flow and number of vessels visualized

Vessel		Control	CMI−	CMI+
SCAo	Change in flow (%)	15.7 ± 14.8	19.1 ± 15.6	5.37 ± 22.3
	# Vessels visualized	20/20	13/13	5/6
IRAo	Change in flow (%)	− 7.03 ± 24.4	12.2 ± 32.5	0.93 ± 26.3
	# Vessels visualized	18/20	12/13	5/6
LRA	Change in flow (%)	3.58 ± 15.4	1.20 ± 21.7	− 18.9 ± 27.4
	# Vessels visualized	19/20	13/13	6/6
RRA	Change in flow (%)	6.97 ± 17.5	− 3.45 ± 18.0	− 25.7 ± 41.2
	# Vessels visualized	20/20	11/13	5/6
SMA	Change in flow (%)	98.8 ± 80.7	65.0 ± 69.0	**25.1 ± 30.2**
	# Vessels visualized	20/20	13/13	6/6
CA	Change in flow (%)	− 3.73 ± 18.9	− 6.29 ± 26.5	15.4 ± 29.7
	# Vessels visualized	19/20	12/13	6/6
SMV	Change in flow (%)	132 ± 80.7	184 ± 151	*49.2 ± 55.9*
	# Vessels visualized	19/20	13/13	6/6
SV	Change in flow (%)	− 4.76 ± 32.3	− 1.83 ± 36.9	− 13.9 ± 18.6
	# Vessels visualized	17/20	13/13	6/6
PV	Change in flow (%)	56.7 ± 47.9	72.1 ± 52.7	*20.4 ± 36.3*
	# Vessels visualized	19/20	13/13	6/6

Percentages are expressed as mean ± 1 standard deviation. Bold indicates statistical significance ($p < 0.05$) compared to controls. Italic indicates statistical significance ($p < 0.05$) between CMI+ and CMI− groups

SCAo supraceliac aorta, *IRAo* infrarenal aorta, *LRA* left renal artery, *RRA* right renal artery, *SMA* superior mesenteric artery, *CA* celiac artery, *SMV* superior mesenteric vein, *SV* splenic vein, *PV* portal vein

LRA and RRA

No significant differences were found between groups for both the LRA and RRA. While not statistically significant, the CMI+ group trended towards decreased LRA percent change in flow values relative to the control group ($p = 0.104$). Similarly, percent change in RRA flow for the CMI+ group trended towards decreased values relative

to the control group ($p = 0.111$) but was not found to be statistically significant.

SMA

While SMA blood flow increased significantly after a meal for control subjects ($p = 5.20e−06$, $d = 1.26$) and for the CMI− group ($p = 0.006$, $d = 0.778$), the CMI+ group did not see a significant increase ($p = 0.473$). Percent change in SMA flow was significantly less in the CMI+ group compared to the control group ($p = 0.002$, $d = − 0.855$) but was not significantly less compared to the CMI− group ($p = 0.102$). Additionally, percent change in flow for the CMI− group was not significantly different from control subjects.

CA

CA blood flow did not increase significantly after a meal for any group, however, preprandial CA flow in the CMI− group was significantly lower than the control group ($p = 0.003$, $d = − 0.553$). While not statistically significant, there was a trend of decreased preprandial CA flow values in the CMI+ group compared to controls ($p = 0.054$).

SMV

SMV blood flow increased significantly after a meal in the control group ($p = 2.51e−08$, $d = 2.10$) and in the CMI− group ($p = 3.49e−06$, $d = 2.15$). The CMI+ group did not see any significant increase in SMV flow after a meal ($p = 0.120$). For the CMI+ group, preprandial SMV flow was significantly higher than the control group ($p = 0.015$, $d = 1.030$) but was not significantly higher than the CMI− group). There was no significant difference in preprandial flow between the control group and the CMI− group. There were also no significant differences in postprandial SMV flow between any of the groups. Percent change in flow for the CMI+ group was significantly less compared to the control group ($p = 0.009$, $d = −0.853$) and the CMI− group ($p = 0.014$, $d = −0.835$).

PV

In control subjects, PV blood flow increased significantly after a meal ($p = 1.17e−05$, $d = 1.137$) as did the CMI− group ($p = 4.90e−05$, $d = 1.724$) while the CMI+ group did not see a significant increase in PV blood flow after a meal). Additionally, percent change in flow for the CMI+ group was significantly less than the control group ($p = 0.037$, $d = -0.604$) and the CMI− group ($p = 0.022$, $d = − 0.808$).

Fig. 3 Average percent changes in blood flow for each subgroup. *indicates statistical significance ($p < 0.05$)

Average Flow Augmentation
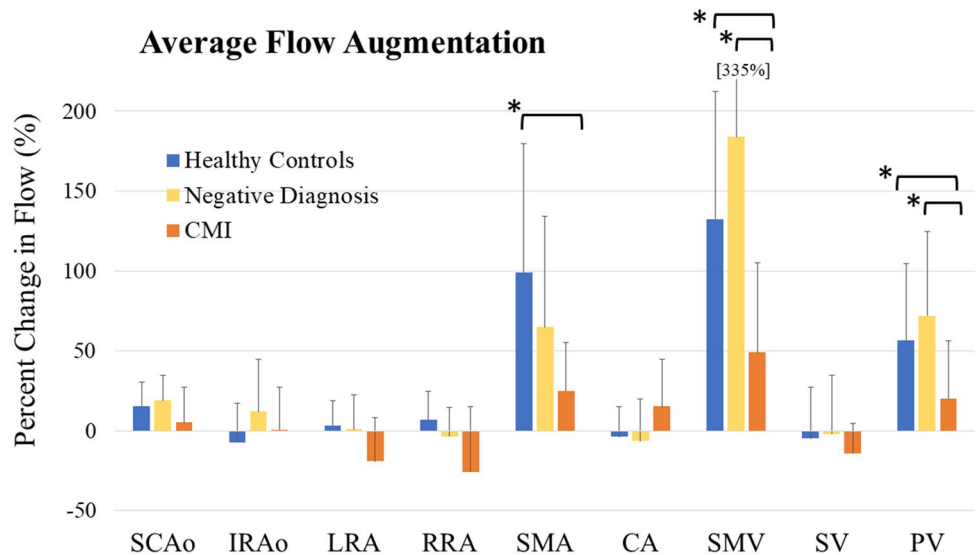
Flow consistency

Correlation analysis was successfully performed on all measured $\bar{Q}_{loss}$ and $\bar{Q}_{branch}$ values, as shown in Fig. 4a. A strong correlation was found between $\bar{Q}_{loss}$ and $\bar{Q}_{branch}$ values ($R^2 = 0.859$). As seen in Fig. 4a, postprandial $\bar{Q}_{loss}$ and $\bar{Q}_{branch}$ values were increased compared to preprandial $\bar{Q}_{loss}$ and preprandial $\bar{Q}_{branch}$ values. This result coincides with observed increases in mesenteric blood flow after a

meal. Correlation analysis was also performed on all measured $\bar{Q}_{PV}$ and $(\bar{Q}_{SV} + \bar{Q}_{SMV})$ values, as shown in Fig. 4b. A strong correlation between $\bar{Q}_{PV}$ and $(\bar{Q}_{SV} + \bar{Q}_{SMV})$ values was also observed ($R^2 = 0.894$). Furthermore, measured volumetric flow rates in this study agreed well with flow rates reported from other imaging modalities [16–19, 22, 29–31, 33–39]. 4D flow rates tended to be closer to those obtained by ultrasound and were consistently higher than those obtained using 2D PC-MRI.
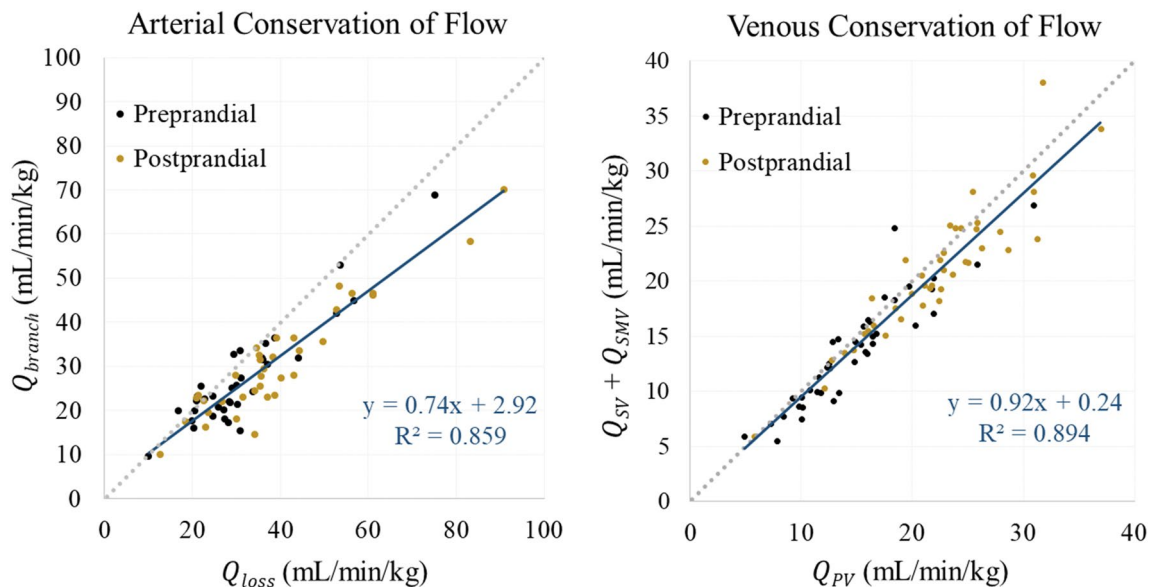

Fig. 4 Correlation analysis of venous and arterial flow measurements. (Left) Difference in blood flow between SCAo and IRAo measurements ($\bar{Q}_{loss}$) plotted against the sum of flow from all branching arteries between the measured SCAo and IRAo segments ($\bar{Q}_{branch}$). The dotted gray line represents true conservation of flow (i.e., one-to-one correlation). (Right) Portal vein flow measurements ($\bar{Q}_{PV}$) plotted against the sum of flow from the splenic and superior mesenteric veins ($\bar{Q}_{SV} + \bar{Q}_{SMV}$)

PC angiograms

PC angiograms were obtained for all 78 pre- and postprandial cases. Locations of likely occlusions, as well as collateral mesenteric vessels, were observed in a variety of patients. Figure 5a shows an example of a patient with median arcuate ligament syndrome in which the median arcuate ligament was compressing the CA. Despite this obstruction, flow in the splenic artery and gastroduodenal artery (GDA) was preserved due to a portion of SMA blood flow being redirected back through the pancreaticoduodenal arcades. The CA could not be visualized on the PC angiogram in this patient. Fasting flow in the GDA was approximately 24.3% of the measured fasting flow in the SMA, which decreased to 7.4% after a meal. However, flow in the SMA and SMV increased to a normal range following a meal (104% and 236%, respectively).

Figure 5b shows a CMI+ patient with a full SMA occlusion (as seen in the PC angiogram) and celiac artery with narrowing. Flow was redirected from the CA to the SMA (just distal to the occlusion) via the pancreaticoduodenal arcades, which were well visualized on the PC angiogram. Distal SMA flow decreased by 7.13% following a meal and SMV flow increased only slightly by 2.93%. Additionally, supplementary collateral flow from the IMA (via Arc of Riolan) was prominent in the angiogram.

Discussion

In this study, 4D flow MRI was used to obtain comprehensive hemodynamic measurements of the mesenteric vasculature in patients suspected of CMI and in control subjects both before and after meal ingestion. Our results were consistent with previous 2D PC-MRI imaging studies [16–19] and demonstrated the potential of 4D flow MRI studies to help disentangle the complex flow patterns observed in CMI. Firstly, 4D flow MRI provides simultaneous acquisition of both hemodynamic information and a PC MRA. Previous studies showed that 3D PC MRA can accurately measure vessel lumens of renal arteries [40] and identify areas of stenoses in suspected chronic mesenteric patients [41]. Secondly, the large volumetric coverage ensures all relevant vessels and collaterals are visualized without the need for a dedicated MRA that often requires injection of a contrast agent. This may be useful since many patients demonstrate significant anatomical variations and may help overcome user- and patient-dependent issues associated with ultrasound. Thirdly, retrospective analysis is possible for any vessel (including collaterals) within the imaging volume without scan time penalty, unlike 2D PC-MRI. Lastly, 4D flow MRI using an accelerated sequence such as PC-VIPR requires only a short 10-min free-breathing scan session while retaining high temporal and spatial resolution.
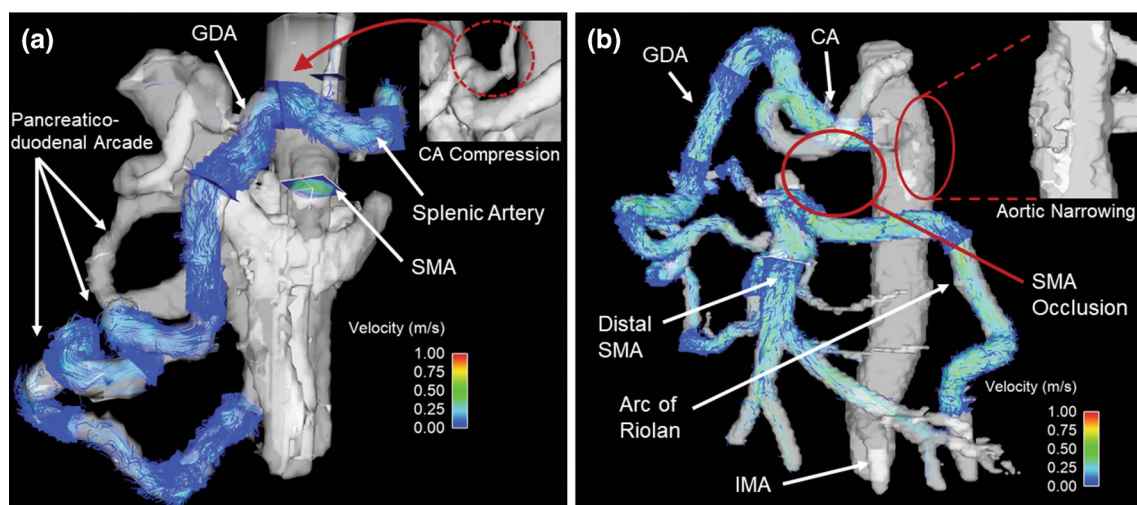

Fig. 5 CA compression (**a**) from median arcuate ligament syndrome with collateral compensation from SMA in a fasting 29-year-old female. Flow from the SMA is redirected through the pancreaticoduodenal arcade to supply the splenic and left gastric branches of the CA. In the PC angiogram, the CA cannot be visualized due to flow obstruction in this vessel. SMA occlusion and celiac narrowing (**b**) in a fasting 42-year-old male with CMI. Numerous collaterals from the IMA, via the Arc of Riolan, and CA, via the pancreaticoduodenal arcades, supply blood to the SMA. The proximal SMA cannot be visualized on the PC angiogram due to the absence of flow. Note that the IMA was included in the field of view in this patient and can be seen at the bottom of the figure. Image inset shows an abnormality in the aorta (situated superoposterior to the celiac root), likely a developing atherosclerotic lesion

Flow consistency

Correlation analysis showed strong correlation between $\bar{Q}_{loss}$ (the difference between SCAo and IRAo flow rates) and $\bar{Q}_{branch}$ (sum of flow rates in vessels exiting between these aortic segments) in both the arterial measurements and venous segments ($\bar{Q}_{PV}$ and $\bar{Q}_{SV} + \bar{Q}_{SMV}$). The slope for both regression models was less than unity, indicating that some flow was not being accounted for in the $\bar{Q}_{branch}$ and $\bar{Q}_{SV} + \bar{Q}_{SMV}$ measurements. This discrepancy is likely due to small, unmeasured collaterals and measurement errors. Despite this, the strong correlation reflects good internal consistency and thus supports the feasibility of 4D flow measurements. Additionally, flow rates in this study agreed well with flow rates reported from other imaging modalities [16–19, 22, 29–31, 33–39].

Flow analysis

Both the control subjects and symptomatic patients without CMI (CMI−) experienced significant blood flow increases in the SMA, SMV, and PV twenty minutes after meal ingestion. This is expected in normal individuals because an increase in SMA flow is needed to satisfy the increased metabolic demands of the gastrointestinal tract [23, 35]. Since a majority of arterial mesenteric flow is returned through the SMV, increases in arterial flow will lead to increases in venous flow in the SMV and subsequently PV, which was observed in this study. Furthermore, an increase in SCAo blood flow was observed in controls and in the CMI− group. This is most likely due to increased cardiac output following meal ingestion, acting to increase volumetric flow rates in the aorta [42]. On the other hand, symptomatic patients with true CMI (CMI+ group) experienced no significant postprandial blood flow increases in any vessel. Furthermore, blood flow responses (percent changes in blood flow) in the SMA, SMV, and PV were significantly decreased in CMI+ patients compared to controls, supporting findings from prior 2D PC-MRI studies [16–19]. In addition, blood flow responses in the SMV and PV were significantly decreased in CMI+ patients compared to the CMI− group, while SMA flow responses were not. SMA flow responses in the CMI− group may be lower due to several patients with narrowing celiac arteries. In these patients, preprandial SMA flow values tended to be higher than in control subjects, which has also been observed in other studies [18, 19]. It should also be noted that, in these patients, SMV and PV flow still increased to normal levels.

Postprandial blood flow increases in the CA were not observed for any group. Since the CA primarily supplies proximal portions of the gastrointestinal tract, blood flow responses occur almost immediately after a meal and return to baseline levels shortly thereafter [23]. In this study, patients were imaged 20 min after ingestion of a meal, allowing postprandial CA flow rates to return to near baseline levels, explaining the negligible observed increases in CA flow rates.

It was also observed that SMV preprandial flow rates were increased in CMI+ patients compared to controls. The explanation for this relationship is not readily apparent. However, similar results were seen in other studies [18, 19] in which average fasting SMV flow rates were slightly higher in diseased patients.

Limitations

Due to the nature of this retrospective study, scans were acquired with 1.5T and 3.0T scanners and with slightly varying imaging protocols. While this might affect image quality, it should have very minor implications on the flow measurements used here. Classifying patients as ischemic versus non-ischemic based on MRA stenoses measurements and follow-up after revascularization may be prone to error due to the lack of a widely accepted gold standard imaging method, which is identified as a major limitation of this study. Specifically, classifying patients with single-vessel disease as CMI− could result in misclassification, as individuals with single-vessel disease have been reported and may see symptom improvement after revascularization. Secondly, it is possible that some CMI+ subjects who have 2 or more significant stenoses but did not undergo revascularization may not see postoperative improvement, suggesting an alternative diagnosis. Additionally, differences in male-to-female ratio within the patient groups may induce measurement bias, as significantly higher flow volumes have been reported in mesenteric arteries of healthy males compared to healthy females [21]. Due to the finite acquisition time of the PC-VIPR pulse sequence (~ 11 min), changes that occur within this digestion phase will not be captured and is noted as an additional limitation.

The post-processing workflow required some manual processing steps such as vessel segmentation and analysis plane placement, decreasing repeatability, and increasing the time required to process cases. This problem could be alleviated by developing an automated pipeline for image segmentation and flow analysis. Despite performing respiratory gating on expiration, patients with median arcuate ligament syndrome may experience more drastic changes in hemodynamic flow patterns while imaged on forced expiration and may be warranted to further evaluate this population. Lastly, a larger patient sample size, particularly a larger CMI+ group, is warranted to further verify the findings in this study.

Future directions

Flow measurements in all 3 main mesenteric arteries (CA, SMA, and IMA) would provide a more comprehensive

analysis of arterial inflow to the small intestine. Because we aimed to measure flow in the SCAo, the IMA was often out of frame even despite the large imaging volume provided by the PC-VIPR sequence used in this study. Flow measurements in this vessel would be particularly valuable in assessing patients with CA and SMA lesions, as the IMA may contribute a large portion of flow via collaterals, such as the Arc of Riolan and the marginal artery of Drummond. Additional information may also be gained by investigating the temporal evolution of blood flow patterns in the primary mesenteric vessels (CA, SMA, and IMA) and collaterals using 4D flow MRI. It has been theorized [43] that gastric hyperemia shortly after meal ingestion causes shunting of blood from the SMA, which may be responsible for the sudden onset of pain (well before food has reached the small intestine) in CMI patients with poor splanchnic blood flow reserve. As noted previously, increases in CA blood flow (gastric hyperemia) occur very soon after meal ingestion [23]. Acquiring multiple 4D flow MRI scans where blood flow changes are measured in the CA, SMA, IMA, and associated collaterals at different points in the digestion phase may provide further insight into the temporal nature of blood flow patterns and the hemodynamic basis for postprandial pain. Accelerated 4D flow MRI approaches such as PC-VIPR are well suited for this type of investigation, and when coupled with advanced, constrained reconstruction techniques, can allow for multiple vessels to be retrospectively analyzed at various points along the digestion phase.

Conclusion

4D flow MRI is a promising non-invasive diagnostic technique that can functionally and anatomically evaluate mesenteric vasculature. 4D flow MRI possesses the unique capability of obtaining complete volumetric hemodynamic information in a single scan, allowing for the quantitative assessment of blood flow patterns in multiple mesenteric vessels, while also producing a high-quality PC angiogram to morphologically assess stenoses and occlusions. The blood flow measurements obtained in this study showed good internal consistency and flow measures were comparable to prior 2D PC-MRI and ultrasound studies measuring mesenteric blood flow. Here, we found quantifiable differences in blood flow hemodynamics in the aorta, SMA, SMV, and PV between individuals diagnosed with CMI, those who were symptomatic but did not have CMI, and control subjects. Additional studies with larger patient cohorts are needed to investigate whether 4D flow MRI can improve the accuracy in the challenging diagnosis of mesenteric ischemia and thereby improve treatment planning and patient care.

Appendix

See Tables 4, 5.

Table 4 Summarized clinical, diagnostic, and follow-up findings for CMI+ subjects

No.	Clinical findings	Diagnostic test findings	Procedures	Follow-up	How was suspicion raised?
1	Currently no symptoms; however, abnormal US findings with suspicion of mesenteric ischemia	US: CA, SMA occlusion. Increase in systolic/diastolic velocity in IMA. MRI: Stable CA and SMA occlusion, reconstitution via pancreaticoduodenal and IMA collaterals. 70% narrowing of the IMA origin	Conservative therapy	Patient remained asymptomatic despite pathological imaging findings. Therapeutic endarterectomy of IMA and bypass to the SMA were proposed, however, patient remained reluctant to pursue the operation	Imaging
2	4 weeks of diarrhea and weight loss, with left-sided postprandial chest pain	CT: Narrowing of CA and SMA. MRI: Hemodynamically significant mesenteric ischemia due to CA and SMA stenosis. SMA stenosis worsened in comparison to previous imaging	SMA and CA PTA with stenting	Postprocedural, symptoms resolved completely	Symptoms/imaging
3	Chronic abdominal discomfort and postprandial pain, nausea, vomiting	CT: Mild SMA and CA stenosis. MRI: moderate-to-severe stenosis at origin of SMA and mild stenosis at origin of CA	Transaortic endarterectomy with mesenteric artery revascularization	Postprocedural, symptoms decreased	Symptoms/imaging
4	Abdominal pain, known Stanford type B aortic dissection	CT: Stanford type B aortic dissection. CA with moderate-to-severe narrowing. MRI: Stable Stanford type B aortic dissection. Moderate-to-severe CA stenosis at the origin	Conservative therapy	Acute abdominal pain improved under conservative therapy. No symptoms indicating chronic SAM ischemia	Imaging
5	Nausea and weight loss. History of thoracoabdominal aneurysm repair, with little to no SMA flow noted during surgery	MRI: Aortic repair. Widely reimplanted CA and IMA, occlusion of SMA with collateral flow. Abnormal flow through the splenic artery, increase in splenic size, and relative flow mismatch to mesenteric arteries, suggestive of mesenteric steal phenomenon	Conservative therapy	Release of symptoms under conservative therapy of transfusion related hemolytic anemia	Symptoms/imaging
6	Weight loss, chronic postprandial pain. History of extensive vascular disease with known CA stenosis	MRI: Non-specific narrowing of proximal CA with distal reconstitution by gastroduodenal artery	Median arcuate ligament surgical release	Postprocedural, complete resolution of postprandial pain. Patient was additionally diagnosed with Takayasu arteritis treated by prednisone	Symptoms/Imaging

CA celiac artery, *SMA* superior mesenteric artery, *IMA* inferior mesenteric artery, *CT* computed tomography, *MRI* magnetic resonance imaging, *US* ultrasound, *PTA* percutaneous transluminal angioplasty, *SAM* segmental arterial mediolysis

Table 5 Summarized clinical, diagnostic, and follow-up findings for CMI– subjects

No.	Clinical findings	Diagnostic test findings	Procedures	Follow-up	How was suspicion raised?
1	Unexplained weight loss and nausea	Endoscopy: choledocholithiasis MRI: choledocholithiasis	Diagnostic testing	Symptom relief after ERCP with sphincterotomy, bile duct stone removal	Symptoms
2	Intermittent nausea, vomiting, weight loss (~3 weeks). Denies abdominal pain or diarrhea	EGD: esophagitis CT: Ectatic aorta. Moderate-to-severe stenosis of CA. Tortuous SMA	Diagnostic testing	Conservative therapy. Symptoms improved on itself	Symptoms
3	Postprandial RUQ pain (>1 year). No weight loss or fear of eating. Underwent cholecystectomy for pain with no improvements	MRCP: Status post cholecystectomy, no new pathological findings	Diagnostic testing	Conservative therapy. History of irritable bowel syndrome, abdominal pain, peptic ulcer, esophageal reflux, difficulty passing stool	Symptoms
4	Postprandial abdominal pain History of abdominal aortic aneurysm post endovascular repair complicated by graft infection	MRI: Stable postoperative changes from distal aortic resection and right axillary to bifemoral bypass graft	Diagnostic testing	Patient continued to have abdominal pain; additional testing revealed that these were linked to inguinal hernia	Symptoms
5	Abdominal pain with occasional nausea. History of laparotomy with median arcuate ligament release, total pancreatectomy, and celiac plexus block	CT: Incomplete opacification of SMV may represent partial thrombosis. Moderate narrowing of CA. Prominent collaterals between mesenteric vessels MRI: SMV patent. Unchanged CA narrowing EGD: Bile gastritis	Diagnostic testing	Conservative therapy of bile gastritis. Given imaging findings, patient would not likely benefit from further release of arcuate ligament	Symptoms/imaging
6	Nausea, constipation, diarrhea. Patient must lay down for couple of hours, otherwise postprandial pain and vomiting	CT: Focal narrowing of SMA may represent non-occlusive thrombus MRI: SMA patent	Diagnostic testing	Conservative therapy. Chronic sphincter of Oddi pain persisted	Symptoms/imaging
7	Follow-up examination in patient with mesenteric steal phenomenon, secondary to hemolytic anemia. History of thoraco-abdominal aneurysm repair, occlusion of SMA	MRI: Patient reimplanted CA and IMA and occluded SMA with collateral circulation. Spleen size decreased	N/A	No symptoms indicating mesenteric ischemia	Imaging
8	Chronic abdominal pain, weight loss. History of median arcuate ligament release, with persistence of symptoms. Possibility of irritable bowel syndrome	MRI: Repaired median arcuate ligament. CA patent without any dynamic compression. SMA and IMA patent	Diagnostic testing	N/A	Symptoms
9	Irritable bowel syndrome symptoms. Diagnostic testing ordered to exclude CMI as a differential diagnosis	MRI: Marked compression of proximal celiac axis with expiration that is only partially relieved with inspiration	Diagnostic testing	N/A	Symptoms
10	Abdominal pain, nausea, vomiting, and weight loss. On imaging, concerns for CA compression syndrome	MRI: Focal compression of CA and signs of hemodynamically significant stenosis from the median arcuate ligament syndrome. Cholelithiasis	Median arcuate ligament surgical release	Postprocedural, no significant improvement of symptoms, persistence of abdominal pain	Symptoms/imaging

Table 5 (continued)

No.	Clinical findings	Diagnostic test findings	Procedures	Follow-up	How was suspicion raised?
11	Right-side abdominal pain radiating to groin. Diagnostic testing ordered to exclude CMI as a differential diagnosis	MRI: ~50% CA stenosis, possible median arcuate ligament compression US abdominal: No testicular mass, probable small fat-containing left inguinal hernia	Diagnostic testing	Findings on MRI were considered incidental with no clinical significance. Symptoms not consistent with MALS	Symptoms
12	Chronic abdominal pain	MRI: High-grade stenosis of CA at origin, partially mitigated during inspiration. Post-stenotic CA dilatation, prominent pancreaticoduodenal arcade. Findings suggest MALS; other etiologies should be considered	Diagnostic testing	Abdominal pain largely resolved. Conservative management of obstructive bowel symptoms with bowel rest and nasogastric tube decompression	Symptoms
13	Abdominal pain, nausea. History of gastric ulcer	MRI: Decreased distance and angle between SMA and aorta suggests SMA syndrome EGD: Hiatal hernia, suggestion of extrinsic compression of duodenum, at the approximate location of the SMA	N/A	N/A	Symptoms/imaging

CMI chronic mesenteric ischemia, *CA* celiac artery, *SMA* superior mesenteric artery, *IMA* inferior mesenteric artery, *CT* computed tomography, *MRI* magnetic resonance imaging, *MRA* magnetic resonance angiography, *US* ultrasound, *MALS* median arcuate ligament syndrome, *EGD* esophagogastroduodenoscopy, *ERCP* endoscopic retrograde cholangiopancreatography, *MRCP* Magnetic resonance cholangiopancreatography, *RUQ* right upper quadrant, *N/A* not applicable

Data availability The datasets used and analyzed during the current study are available from the corresponding author on reasonable request. Code availability Not applicable.

Compliance with ethical standards

Conflict of interest The University of Wisconsin - Madison receives research support from GE Healthcare. The authors declare that they have no other potential competing interests.

Ethics approval All procedures performed in studies involving human participants were in accordance with the ethical standards of the institutional research committee and with the 1964 Helsinki declaration and its later amendments or comparable ethical standards. Patients suspected of CMI were scanned for clinical purposes and a University of Wisconsin - Madison Health Sciences IRB approved protocol (PI: Scott Reeder, MD, PhD; Title: Clinical Imaging and Outcomes Research; IRB Tracking Number: 2016-0518) was used to retrospectively analyze those datasets. A separate IRB protocol (PI: Scott Reeder, MD, PhD; Title: Evaluation of Liver Hemodynamics by 5-point 4D Phase Contrast MRA; IRB Tracking Number: H-2010-0035) was used for the prospective recruitment and imaging of healthy volunteers and was approved by the University of Wisconsin - Madison Health Sciences Institutional Review Board. All IRB protocols were compliant with the Health Insurance Portability and Accountability Act (HIPAA).

Consent to participate Informed consent was obtained from all healthy control participants included in the study. Need for consent from the patient cohorts was waived.

Consent for publication Not applicable.

References

1. van Bockel JH, Geelkerken RH, Wasser MN (2001) Chronic splanchnic ischaemia. Best Pract Res Clin Gastroenterol 15 (1):99-119. https://doi.org/10.1053/bega.2001.0158

2. Kolkman JJ, Geelkerken RH (2017) Diagnosis and treatment of chronic mesenteric ischemia: An update. Best Pract Res Clin Gastroenterol 31 (1):49-57. https://doi.org/10.1016/j.bpg.2017.01.003

3. Sreenarasimhaiah J (2005) Chronic mesenteric ischemia. Best Pract Res Clin Gastroenterol 19 (2):283-295. https://doi.org/10.1016/j.bpg.2004.11.002

4. Pillai AK, Kalva SP, Hsu SL, Walker TG, Silberzweig JE, Annamalai G, Baerlocher MO, Mitchell JW, Midia M, Nikolic B, Dariushnia SR (2018) Quality Improvement Guidelines for Mesenteric Angioplasty and Stent Placement for the Treatment of Chronic Mesenteric Ischemia. J Vasc Interv Radiol 29 (5):642-647. https://doi.org/10.1016/j.jvir.2017.11.024

5. Terlouw LG, Moelker A, Abrahamsen J, Acosta S, Bakker OJ, Baumgartner I, Boyer L, Corcos O, van Dijk LJ, Duran M, Geelkerken RH, Illuminati G, Jackson RW, Kärkkäinen JM, Kolkman JJ, Lönn L, Mazzei MA, Nuzzo A, Pecoraro F, Raupach J, Verhagen HJ, Zech CJ, van Noord D, Bruno MJ (2020) European guidelines on chronic mesenteric ischaemia – joint United European Gastroenterology, European Association for Gastroenterology, Endoscopy and Nutrition, European Society of Gastrointestinal and Abdominal Radiology, Netherlands Association of Hepatogastroenterologists, Hellenic Society of Gastroenterology, Cardiovascular and Interventional Radiological Society of Europe, and Dutch Mesenteric Ischemia Study group clinical guidelines on the diagnosis and treatment of patients with chronic mesenteric ischaemia. United European Gastroenterol J 8 (4):371-395. https://doi.org/10.1177/2050640620916681

6. Oliva IB, Davarpanah AH, Rybicki FJ, Desjardins B, Flamm SD, Francois CJ, Gerhard-Herman MD, Kalva SP, Ashraf Mansour M, Mohler ER, 3rd, Schenker MP, Weiss C, Dill KE (2013) ACR Appropriateness Criteria (R) imaging of mesenteric ischemia. Abdom Imaging 38 (4):714-719. https://doi.org/10.1007/s00261-012-9975-2

7. Amin MA, Nooman NA, Moussa GI (2014) Acute and chronic mesenteric ischemia: Multidetector CT and CT angiographic findings. The Egyptian Journal of Radiology and Nuclear Medicine 45 (4):1063-1070. https://doi.org/10.1016/j.ejrnm.2014.06.001

8. Mazzei MA, Guerrini S, Cioffi Squitieri N, Vindigni C, Imbriaco G, Gentili F, Berritto D, Mazzei FG, Grassi R, Volterrani L (2016) Reperfusion in non-occlusive mesenteric ischaemia (NOMI): effectiveness of CT in an emergency setting. Br J Radiol 89 (1061):20150956-20150956. https://doi.org/10.1259/bjr.20150956

9. Carlos RC, Stanley JC, Stafford-Johnson D, Prince MR (2001) Interobserver variability in the evaluation of chronic mesenteric ischemia with gadolinium-enhanced MR angiography. Acad Radiol 8 (9):879-887. https://doi.org/10.1016/s1076-6332(03)80767-5

10. Meaney JF, Prince MR, Nostrant TT, Stanley JC (1997) Gadolinium-enhanced MR angiography of visceral arteries in patients with suspected chronic mesenteric ischemia. J Magn Reson Imaging 7 (1):171-176. https://doi.org/10.1002/jmri.1880070126

11. Mazzei MA, Guerrini S, Cioffi Squitieri N, Imbriaco G, Chieca R, Civitelli S, Savelli V, Mazzei FG, Volterrani L (2013) Magnetic resonance imaging: is there a role in clinical management for acute ischemic colitis? World journal of gastroenterology 19 (8):1256-1263. https://doi.org/10.3748/wjg.v19.i8.1256

12. Zwolak RM, Fillinger MF, Walsh DB, LaBombard FE, Musson A, Darling CE, Cronenwett JL (1998) Mesenteric and celiac duplex scanning: a validation study. J Vasc Surg 27 (6):1078-1087; discussion 1088. https://doi.org/10.1016/s0741-5214(98)60010-0

13. Muller AF (1992) Role of duplex Doppler ultrasound in the assessment of patients with postprandial abdominal pain. Gut 33 (4):460-465. https://doi.org/10.1136/gut.33.4.460

14. Gentile AT, Moneta GL, Lee RW, Masser PA, Taylor LM, Jr., Porter JM (1995) Usefulness of fasting and postprandial duplex ultrasound examinations for predicting high-grade superior mesenteric artery stenosis. Am J Surg 169 (5):476-479. https://doi.org/10.1016/s0002-9610(99)80198-6

15. Sabba C, Ferraioli G, Sarin SK, Lerner E, Groszmann RJ, Taylor KJ (1990) Feasibility spectrum for Doppler flowmetry of splanchnic vessels. In normal and cirrhotic populations. J Ultrasound Med 9 (12):705-710. https://doi.org/10.7863/jum.1990.9.12.705

16. Li KC, Whitney WS, McDonnell CH, Fredrickson JO, Pelc NJ, Dalman RL, Jeffrey RB, Jr. (1994) Chronic mesenteric ischemia: evaluation with phase-contrast cine MR imaging. Radiology 190 (1):175-179. https://doi.org/10.1148/radiology.190.1.8259400

17. Burkart DJ, Johnson CD, Reading CC, Ehman RL (1995) MR measurements of mesenteric venous flow: prospective evaluation in healthy volunteers and patients with suspected chronic mesenteric ischemia. Radiology 194 (3):801-806. https://doi.org/10.1148/radiology.194.3.7862982

18. Li KC, Hopkins KL, Dalman RL, Song CK (1995) Simultaneous measurement of flow in the superior mesenteric vein and artery with cine phase-contrast MR imaging: value in diagnosis of chronic mesenteric ischemia. Work in progress. Radiology 194 (2):327-330. https://doi.org/10.1148/radiology.194.2.7824706

19. Dalman RL, Li KC, Moon WK, Chen I, Zarins CK (1996) Diminished postprandial hyperemia in patients with aortic and mesenteric arterial occlusive disease. Quantification by magnetic resonance flow imaging. Circulation 94 (9 Suppl):Ii206-210

20. Roldan-Alzate A, Francois CJ, Wieben O, Reeder SB (2016) Emerging Applications of Abdominal 4D Flow MRI. AJR Am J Roentgenol 207 (1):58-66. https://doi.org/10.2214/ajr.15.15995

21. Siedek F, Giese D, Weiss K, Ekdawi S, Brinkmann S, Schroeder W, Bruns C, Chang DH, Persigehl T, Maintz D, Haneder S (2018) 4D flow MRI for the analysis of celiac trunk and mesenteric artery stenoses. Magn Reson Imaging 53:52-62. https://doi.org/10.1016/j.mri.2018.06.021

22. Roldan-Alzate A, Frydrychowicz A, Said A, Johnson KM, Francois CJ, Wieben O, Reeder SB (2015) Impaired regulation of portal venous flow in response to a meal challenge as quantified by 4D flow MRI. J Magn Reson Imaging 42 (4):1009-1017. https://doi.org/10.1002/jmri.24886

23. Someya N, Endo MY, Fukuba Y, Hayashi N (2008) Blood flow responses in celiac and superior mesenteric arteries in the initial phase of digestion. Am J Physiol Regul Integr Comp Physiol 294 (6):R1790-1796. https://doi.org/10.1152/ajpregu.00553.2007

24. Gu T, Korosec FR, Block WF, Fain SB, Turk Q, Lum D, Zhou Y, Grist TM, Haughton V, Mistretta CA (2005) PC VIPR: a high-speed 3D phase-contrast method for flow quantification and high-resolution angiography. AJNR Am J Neuroradiol 26 (4):743-749

25. Johnson KM, Markl M (2010) Improved SNR in phase contrast velocimetry with five-point balanced flow encoding. Magn Reson Med 63 (2):349-355. https://doi.org/10.1002/mrm.22202

26. Liu J, Redmond MJ, Brodsky EK, Alexander AL, Lu A, Thornton FJ, Schulte RF, Grist TM, Pipe JG, Block WF (2006) Generation and visualization of four-dimensional MR velocity data using an undersampled 3-D projection trajectory. IEEE Trans Med Imaging 25 (2):148-157. https://doi.org/10.1109/tmi.2005.861706

27. Walker PG, Cranney GB, Scheidegger MB, Waseleski G, Pohost GM, Yoganathan AP (1993) Semiautomated method for noise reduction and background phase error correction in MR phase velocity data. J Magn Reson Imaging 3 (3):521-530. https://doi.org/10.1002/jmri.1880030315

28. Stalder AF, Russe MF, Frydrychowicz A, Bock J, Hennig J, Markl M (2008) Quantitative 2D and 3D phase contrast MRI: optimized analysis of blood flow and vessel wall parameters. Magn Reson Med 60 (5):1218-1231. https://doi.org/10.1002/mrm.21778

29. Burkart DJ, Johnson CD, Ehman RL (1993) Correlation of arterial and venous blood flow in the mesenteric system based on MR findings. 1993 ARRS Executive Council Award. AJR Am J Roentgenol 161 (6):1279-1282. https://doi.org/10.2214/ajr.161.6.8249742

30. Burkart DJ, Johnson CD, Morton MJ, Wolf RL, Ehman RL (1993) Volumetric flow rates in the portal venous system: measurement with cine phase-contrast MR imaging. AJR Am J Roentgenol 160 (5):1113-1118. https://doi.org/10.2214/ajr.160.5.8470589

31. Moriyasu F, Ban N, Nishida O, Nakamura T, Miyake T, Uchino H, Kanematsu Y, Koizumi S (1986) Clinical application of an ultrasonic duplex system in the quantitative measurement of portal blood flow. J Clin Ultrasound 14 (8):579-588. https://doi.org/10.1002/jcu.1870140802

32. Cohen J (1988) Statistical power analysis for the behavioral sciences. L. Erlbaum Associates, Hillsdale, N.J.

33. Les AS, Yeung JJ, Schultz GM, Herfkens RJ, Dalman RL, Taylor CA (2010) Supraceliac and Infrarenal Aortic Flow in Patients with Abdominal Aortic Aneurysms: Mean Flows, Waveforms, and Allometric Scaling Relationships. Cardiovasc Eng Technol 1 (1). https://doi.org/10.1007/s13239-010-0004-8

34. Taylor CA, Cheng CP, Espinosa LA, Tang BT, Parker D, Herfkens RJ (2002) In vivo quantification of blood flow and wall shear stress in the human abdominal aorta during lower limb exercise. Ann Biomed Eng 30 (3):402-408. https://doi.org/10.1114/1.1476016

35. Sieber C, Beglinger C, Jaeger K, Hildebrand P, Stalder GA (1991) Regulation of postprandial mesenteric blood flow in humans: evidence for a cholinergic nervous reflex. Gut 32 (4):361-366. https://doi.org/10.1136/gut.32.4.361

36. Moneta GL, Taylor DC, Helton WS, Mulholland MW, Strandness DE, Jr. (1988) Duplex ultrasound measurement of postprandial intestinal blood flow: effect of meal composition. Gastroenterology 95 (5):1294-1301. https://doi.org/10.1016/0016-5085(88)90364-2

37. Cooper AM, Braatvedt GD, Qamar MI, Brown H, Thomas DM, Halliwell M, Read AE, Corrall RJ (1991) Fasting and post-prandial splanchnic blood flow is reduced by a somatostatin analogue (octreotide) in man. Clin Sci (Lond) 81 (2):169-175. https://doi.org/10.1042/cs0810169

38. Nishida O, Moriyasu F, Nakamura T, Ban N, Miura K, Sakai M, Uchino H, Miyake T (1987) Interrelationship between splenic and superior mesenteric venous circulation manifested by transient splenic arterial occlusion using a balloon catheter. Hepatology 7 (3):442-446. https://doi.org/10.1002/hep.1840070305

39. Gaiani S, Bolondi L, Bassi SL, Santi V, Zironi G, Barbara L (1989) Effect of meal on portal hemodynamics in healthy humans and in patients with chronic liver disease. Hepatology 9 (6):815-819. https://doi.org/10.1002/hep.1840090604

40. Francois CJ, Lum DP, Johnson KM, Landgraf BR, Bley TA, Reeder SB, Schiebler ML, Grist TM, Wieben O (2011) Renal arteries: isotropic, high-spatial-resolution, unenhanced MR angiography with three-dimensional radial phase contrast. Radiology 258 (1):254-260. https://doi.org/10.1148/radiol.10100443

41. Wasser MN, Geelkerken RH, Kouwenhoven M, van Bockel JH, Hermans J, Schultze Kool LJ, de Roos A (1996) Systolically gated 3D phase contrast MRA of mesenteric arteries in suspected mesenteric ischemia. J Comput Assist Tomogr 20 (2):262-268. https://doi.org/10.1097/00004728-199603000-00017

42. Waaler BA, Eriksen M, Toska K (1991) The effect of meal size on postprandial increase in cardiac output. Acta Physiol Scand 142 (1):33-39. https://doi.org/10.1111/j.1748-1716.1991.tb09125.x

43. Poole JW, Sammartano RJ, Boley SJ (1987) Hemodynamic basis of the pain of chronic mesenteric ischemia. Am J Surg 153 (2):171-176. https://doi.org/10.1016/0002-9610(87)90809-9